Published in final edited form as:
J Neurosurg. 2011 March ; 114(3): 595–603. doi:10.3171/2010.2.JNS091322.

Coregistered fluorescence-enhanced tumor resection of malignant glioma: relationships between δ-aminolevulinic acid–induced protoporphyrin IX fluorescence, magnetic resonance imaging enhancement, and neuropathological parameters

David W. Roberts, M.D.[1,2,5], **Pablo A. Valdés, B.S.**[2,3], **Brent T. Harris, M.D., Ph.D.**[2,4], **Kathryn M. Fontaine, B.S.E.**[3], **Alexander Hartov, Ph.D.**[3,5], **Xiaoyao Fan, B.E.**[3], **Songbai Ji, D.Sc.**[3], **S. Scott Lollis, M.D.**[1], **Brian W. Pogue, Ph.D.**[3,5], **Frederic Leblond, Ph.D.**[3], **Tor D. Tosteson, Sc.D.**[2,5], **Brian C. Wilson, Ph.D.**[6], and **Keith D. Paulsen, Ph.D.**[2,3,5]

[1]Section of Neurosurgery, Dartmouth-Hitchcock Medical Center, Lebanon

[4]Department of Pathology, Dartmouth-Hitchcock Medical Center, Lebanon

[5]Norris Cotton Cancer Center, Dartmouth-Hitchcock Medical Center, Lebanon

[2]Dartmouth Medical School Dartmouth College, Hanover, New Hampshire

[3]Thayer School of Engineering, Dartmouth College, Hanover, New Hampshire

[6]Department of Medical Biophysics, University of Toronto, Ontario Cancer Institute, Princess Margaret Hospital, Toronto, Ontario, Canada

Abstract

Object—The aim of this study was to investigate the relationships between intraoperative fluorescence, features on MR imaging, and neuropathological parameters in 11 cases of newly diagnosed glioblastoma multiforme (GBM) treated using protoporphyrin IX (PpIX) fluorescence-guided resection.

Methods—In 11 patients with a newly diagnosed GBM, δ-aminolevulinic acid (ALA) was administered to enhance endogenous synthesis of the fluorophore PpIX. The patients then underwent fluorescence-guided resection, coregistered with conventional neuronavigational image guidance. Biopsy specimens were collected at different times during surgery and assigned a fluorescence level of 0–3 (0, no fluorescence; 1, low fluorescence; 2, moderate fluorescence; or 3, high fluorescence). Contrast enhancement on MR imaging was quantified using two image metrics: 1) Gd-enhanced signal intensity (GdE) on T1-weighted subtraction MR image volumes, and 2) normalized contrast ratios (nCRs) in T1-weighted, postGd-injection MR image volumes for each biopsy specimen, using the biopsy-specific image-space coordinate transformation provided

Address correspondence to: David W. Roberts, M.D., Section of Neurosurgery, Dartmouth-Hitchcock Medical Center, One Medical Center Drive, Lebanon, New Hampshire 03756. David.W.Roberts@dartmouth.edu..

Author contributions to the study and manuscript preparation include the following. Conception and design: DW Roberts, A Hartov, BW Pogue, KD Paulsen. Acquisition of data: DW Roberts, PA Valdés, BT Harris, KM Fontaine, A Hartov, X Fan, S Ji, SS Lollis, F Leblond, KD Paulsen. Analysis and interpretation of data: DW Roberts, PA Valdés, BT Harris, TD Tosteson, BC Wilson, KD Paulsen. Drafting the article: DW Roberts, PA Valdés, BT Harris, BW Pogue, F Leblond, BC Wilson, KD Paulsen. Critically revising the article: DW Roberts, PA Valdés, KD Paulsen. Reviewed final version of the manuscript and approved it for submission: DW Roberts, PA Valdés, BT Harris, KM Fontaine, A Hartov, X Fan, S Ji, SS Lollis, BW Pogue, F Leblond, TD Tosteson, BC Wilson, KD Paulsen. Statistical analysis: PA Valdés, TD Tosteson. Administrative/technical/material support: KM Fontaine, X Fan, S Ji. Study supervision: DW Roberts, KD Paulsen.

Portions of this work were presented at the 77th Annual Meeting of the American Association of Neurological Surgeons in San Diego, California, on May 5, 2009.

by the navigation system. Subsequently, each GdE and nCR value was grouped into one of two fluorescence categories, defined by its corresponding biopsy specimen fluorescence assessment as negative fluorescence (fluorescence level 0) or positive fluorescence (fluorescence level 1, 2, or 3). A single neuropathologist analyzed the H & E–stained tissue slides of each biopsy specimen and measured three neuropathological parameters: 1) histopathological score (0–IV); 2) tumor burden score (0–III); and 3) necrotic burden score (0–III).

Results—Mixed-model analyses with random effects for individuals show a highly statistically significant difference between fluorescing and nonfluorescing tissue in GdE (mean difference 8.33, $p = 0.018$) and nCRs (mean difference 5.15, $p < 0.001$). An analysis of association demonstrated a significant relationship between the levels of intraoperative fluorescence and histopathological score ($\chi^2 = 58.8$, $p < 0.001$), between fluorescence levels and tumor burden ($\chi^2 = 42.7$, $p < 0.001$), and between fluorescence levels and necrotic burden ($\chi^2 = 30.9$, $p < 0.001$). The corresponding Spearman rank correlation coefficients were 0.51 ($p < 0.001$) for fluorescence and histopathological score, and 0.49 ($p < 0.001$) for fluorescence and tumor burden, suggesting a strongly positive relationship for each of these variables.

Conclusions—These results demonstrate a significant relationship between contrast enhancement on preoperative MR imaging and observable intraoperative PpIX fluorescence. The finding that preoperative MR image signatures are predictive of intraoperative PpIX fluorescence is of practical importance for identifying candidates for the procedure. Furthermore, this study provides evidence that a strong relationship exists between tumor aggressiveness and the degree of tissue fluorescence that is observable intraoperatively, and that observable fluorescence has an excellent positive predictive value but a low negative predictive value.

Keywords

δ-aminolevulinic acid; contrast enhancement; fluorescence-guided resection; malignant glioma; protoporphyrin IX

Interest in the clinical use of fluorescence guidance for resection of malignant gliomas, meningiomas, and metastatic brain tumors has grown over the last decade.5,8,10,12–16,21,23,24,26–33,35 Trials of fluorescein sodium to produce intraoperative fluorescence for resection of brain tumors were first reported in 1948 by Moore et al.,20 and later, in 1982, by Murray.22 More recently, fluorescence guidance has taken advantage of intrinsic metabolic and structural changes that occur within tumors by exploiting the heme biosynthetic pathway and a natural biochemical precursor in that pathway, ALA.8,21,28–33,35 Exogenous administration of ALA overloads the heme pathway and leads to selective accumulation of the fluorescent heme precursor PpIX in neoplastic tissues.4,7,11 Accumulated PpIX levels are sufficiently high that neoplastic tissue can be easily visualized through a surgical microscope adapted to excite PpIX fluorescence.32

By far the largest and most important experience described to date in which ALA-induced PpIX fluorescence was used for intraoperative resection guidance has been the pioneering work of Stummer and the ALA-Glioma Study Group in Germany. They have reported in a series of publications that: 1) complete resection of contrast-enhancing tumor occurred in a greater proportion of patients undergoing FGR compared with standard white-light surgery (65% vs 36%); 2) a significantly longer 6-month progression-free survival was achieved in the FGR group than in the control group (41% vs 21.1%)29; 3) after accounting for selection and other biases, a statistically significant survival advantage for complete versus incomplete resection was seen (median survival time of 16.9 months vs 11.8 months, $p < 0.0001$);24,30 and 4) a significant association existed between residual contrast on postoperative MR imaging and residual intraoperative fluorescence.28 In addition to the

work in Germany, other studies have reported experiences in regard to the uses and limitations of the technology.19,37,39

We hypothesize a correlation between conventional features from coregistered preoperative MR imaging and intraoperative fluorescence as well as a correlation between neuropathological parameters and intraoperative fluorescence. In this study we provide initial findings from coregistered ALA-induced PpIX fluorescence–enhanced resection of malignant gliomas in 11 patients with newly diagnosed GBM, under an Institutional Review Board–approved FDA Investigational New Drug protocol, with the goal of establishing the statistical significance of relationships between 1) quantitative assessments of MR image signals and the spatially coregistered qualitative fluorescence signatures determined intraoperatively, and 2) these same qualitative fluorescence determinations and subsequent neuropathological evaluations of the biopsy specimens taken from these locations.

Methods

Patient Selection

This study was approved by our Institutional Review Board, and informed consent was obtained from all patients. Patients with a new pathological diagnosis of GBM who underwent operations in accordance with our fluorescence-guided tumor resection protocol were included in this study. These patients were part of a larger group, inclusion criteria for which were as follows: 1) preoperative diagnosis of presumed low- or high-grade glioma; 2) tumor judged to be suitable for open cranial resection based on preoperative imaging studies; 3) age 18 years or older; and 4) ability to provide informed consent. Exclusion criteria were as follows: 1) pregnancy or breastfeeding; 2) history of cutaneous photosensitivity, hypersensitivity to porphyrins, photodermatosis, exfoliative dermatitis, or porphyria; 3) history of liver disease within the last 12 months; 4) ALT, AST, ALP, or bilirubin levels > 2.5 times the normal limit at any time during the previous 2 months; 5) plasma creatinine > 180 μmol/L; 6) inability to comply with the photosensitivity precautions associated with the study; and 7) serious associated psychiatric illness. Between August 2008 and April 2009, a total of 24 patients were enrolled, 11 of whom were newly diagnosed with GBM and were the subject of this analysis. They were chosen because they shared a common diagnosis which has been the subject of previous investigations of ALA-induced PpIX FGR. Diagnoses in the remaining 13 patients were as follows: 3 dysembryoplastic neuroepithelial tumors (Grade I), 1 ganglioglioma (Grade I), 1 anaplastic mixed oligoastrocytoma (Grade III), 1 anaplastic oligodendroglioma (Grade III), 2 anaplastic astrocytomas (Grade III), 2 recurrent GBMs (Grade IV), 1 gliosarcoma (Grade IV), and 2 vascular malformations. Table 1 summarizes the characteristics of the 11 patients studied.

Surgical Procedure

Patients were administered an oral dose of 20 mg/kg body weight ALA (DUSA Pharmaceuticals) dissolved in 100 ml of water approximately 3 hours prior to the induction of anesthesia. Preoperative, high-resolution, contrast-enhanced, T1-weighted axial MR images (256 × 256 matrix, 124 axial slices, 1.5-mm slice thickness, TE 3 msec, TR 25 msec; 0.1 mmol/kg body weight Gd-diethylenetriamine pentaacetic acid) were acquired for each participant on the day of the procedure. The operating room was equipped with a Zeiss OPMI Pentero operating microscope (Carl Zeiss Surgical GmbH) enabled with fluorescence imaging and a StealthStation Treon (Medtronic) for neurosurgical navigation. The Zeiss OPMI Pentero operating microscope was modified to include a blue light source for excitation (that is, a wavelength of 400 nm) and a 620–710 nm BP filter for recording PpIX fluorescence on a sensitive 3-chip charge-coupled device camera. The patient's head was

positioned in 3-point pin fixation, registered with the image-guidance system by using scalp-based fiducials, and then prepared and draped following standard practice. The Pentero microscope was coregistered with the navigational system and surgical field, such that the focal point of the microscope was mapped to the patient coordinate system in the operating room, and its coordinates were displayed in image-space on the StealthStation image-guidance monitor.

The primary guide for resection was conventional neurosurgical technique with white light illumination, assisted by neuronavigational guidance. Only tissue judged to be reasonably part of the planned resection volume, or judged to be abnormal tissue by other assessments (that is, texture, nonfluorescent color, and so on) was included in the resection. In no instance was tissue resected on the basis of fluorescence alone. At different times during resection, the surgeon switched to blue-light excitation mode and red-shifted-filtered collection to visualize fluorescence. Biopsy specimens from image-registered sites within the intended resection volume were collected at the beginning, middle, and end of resection, and digital images in white- and blue-light modes were recorded concurrently for each biopsy acquisition. Biopsy sites were assigned a fluorescence level by the study surgeon (D.W.R.) consisting of the following scores: 0, no fluorescence; 1, low fluorescence; 2, moderate fluorescence; or 3, high fluorescence. For each patient, biopsy specimens were collected in both fluorescing and nonfluorescing regions within the preoperatively planned resection volume.

Each excised specimen was immediately separated into three equal parts for further processing, as follows: 1) one part was placed in formalin; 2) a second part was placed in Optimal Cutting Temperature compound and frozen in liquid nitrogen; and 3) the third part was placed in a cryogenic vial and also frozen in liquid nitrogen. For each biopsy specimen, we retrieved the corresponding image-space coordinates provided by the navigational system and matched the coordinates to the corresponding blue- and white-light digital images (Fig. 1). Resection of tumor was continued until the surgeon judged from both the image-guidance and surgical microscope systems that no more malignant tissue that could be safely removed was present.

Neuropathological Investigation

Neuropathological analysis was performed on formalin-fixed, paraffin-embedded biopsy tissue processed for H & E staining. A single neuropathologist (B.T.H.) analyzed the H & E–stained tissue slides while blinded to the pathological diagnoses derived from the main surgical specimen in each case. Three major histological parameters were measured: 1) histopathological score; 2) tumor burden; and 3) necrotic burden. Each H & E–stained tissue section was assigned a histopathological score (0–IV) based on the current WHO grading criteria for the particular neoplasms observed.18 The following histopathological characteristics were used for each of the biopsy specimens and judged independently regardless of the overall WHO grade assigned: 0, normal or fully necrotic tissue section with no viable tumor cells observed; I, tissue section with diffusely infiltrating tumor cells (reserved for specific types of glial or glioneuronal neoplasms such as pilocytic astrocytomas, dysembryoplastic neuroepithelial tumors, and gangliogliomas); II, tissue section with a higher number of diffusely infiltrating, pleomorphic cells and no observable necrosis, mitotic figures, or endothelial proliferation; III, tissue section with highly pleomorphic tumor cells, with mitotic figures and no observable necrosis or endothelial proliferation; and IV, tissue section with highly pleomorphic tumor cells, with mitotic figures and either observable necrosis and/or endothelial proliferation. In addition, the tumor burden (0–III) for each tissue section was assessed and defined on the basis of the percentage of area occupied by tumor compared with nontumor cells in each tissue slide (as estimated by 2 observers, B.T.H. and P.V.). The following tumor burden scores were

assigned: 0, normal or fully necrotic tissue section with no observable or viable tumor cells; I, > 0% and ≤ 33% viable tumor; II, > 33% and ≤ 67% viable tumor; and III, > 67% viable tumor. Necrotic burden (0–III) for each tissue section was assessed and defined on the basis of the percentage of area occupied by necrotic tissue compared with nonnecrotic tissue in each slide (as estimated by 2 observers, B.T.H. and P.V.). The following necrotic burden scores were assigned: 0, no observable necrosis; I, > 0% and ≤ 33% necrosis; II, > 33% and ≤ 67% necrosis; and III, > 67% necrosis.

Data Analysis and Image Processing

Results for each biopsy specimen were arranged according to fluorescence level (0–3), histopathological score, tumor burden, and necrotic burden in 2-way tables of association. Sensitivities, specificities, PPVs, NPVs, and odds ratios for fluorescence score were calculated to summarize the strength of association in these tables (Table 2). A chi-square statistic was used to estimate the significance of a relationship between fluorescence, histopathological score, tumor burden, and necrotic burden (Table 3). The Spearman rank correlation coefficient was calculated to summarize the strength of these relationships.

The following image measures of contrast enhancement on MR imaging were used: 1) GdE and 2) nCR. The GdE values refer to the absolute MR imaging signal intensity of a T1-weighted subtraction image volume; that is, postcontrast image volume minus precontrast-injection image volume. Eight MR imaging subtraction image volumes were used in the analysis for GdE (high-resolution T1-weighted image volumes prior to Gd injection were not available in 3 cases). The average MR imaging signal intensity value of a 3 × 3 × 1 voxel (2.8 × 2.8 × 1.5 mm) centered about the specific image-space coordinates for each biopsy specimen was calculated from the patient-specific subtraction image volume to determine the GdE value.

The nCR, a well-established imaging parameter,25 was also used as a metric for MR imaging signal contrast enhancement, according to the following formula:

$$nCR = (SI_b - SI_n) / SI_{bg}$$

where SI_b the refers to the MR imaging signal intensity of the image-space coordinates corresponding to a biopsy specimen; SI_n refers to a weighted average MR imaging signal intensity of gray and white matter; SI_{bg} refers to an average MR imaging signal intensity of background (in air). We used MATLAB software (Version R2008b; The Mathworks, Inc.) to automatically calculate the contrast of the voxel in the T1-weighted, postGd-injection image volume corresponding to each biopsy specimen, using the biopsy-specific image-space coordinate transformation provided by the navigation system. Briefly, the average MR imaging signal intensity value of a 3 × 3 × 1 voxel (2.8 × 2.8 × 1.5 mm) centered about the specific image-space coordinates for each biopsy specimen was calculated to determine the SI_b values. The weighted-average MR imaging signal intensity value of a 5 × 5 × 3 voxel (4.7 × 4.7 × 4.5 mm) of gray and white matter was calculated to determine the corresponding SI_n values. The average MR imaging signal intensity value of an 11 × 11 × 3 voxel (10.3 × 10.3 × 4.5 mm) of space outside the patient's head was calculated to determine the SI_{bg} values.

After calculating the voxel GdE and nCR values in the image volume, a systematic ROI thresholding was performed to improve the accuracy of the navigational information by allowing for the occurrence of intraoperative brain shift. On an axial image, an ROI with a radius of 3 pixels (2.8 mm) centered about the specific image-space coordinates for each biopsy specimen was calculated. All ROIs that did not encompass two (or more) grossly

distinct tissue regions as visualized on the coregistered MR imaging (for example, necrotic core, contrast-enhancing rim of the tumor, or white matter) were used in the final analysis. Subsequently, each specimen with its corresponding fluorescence level was automatically matched to the corresponding specimen's GdE and nCR values, which were then grouped into a binary system of negative fluorescence (level 0) or positive fluorescence (level 1, 2, or 3). To accommodate the multiple samples per person, mixed models6 with random effects for the individual were used to assess a difference in GdE and nCR values between the positive and negative fluorescence groups. The 95% CIs of the mean GdE and nCR for the positive and negative fluorescence groups were calculated and plotted. Tumor volume for each patient was determined by manual segmentation of the region enclosed by contrast-enhancing tissue on T1-weighted MR image volumes. A p value of < 0.05 was considered statistically significant for all tests. Statistical analyses were performed with Stata 10.0 software (StataCorp LP).

Results

Association Between Intraoperative Fluorescence and MR Image Measures

The 95% CIs of the mean GdE and nCR for the fluorescent and nonfluorescent groups are plotted in Fig. 2. For GdE, the mean difference was 8.33 (95% CI 1.42–15.24, $p = 0.018$), and for nCR the mean difference was 5.15 (95% CI 2.54–7.77, $p < 0.001$). These results demonstrate a highly statistically significant difference in GdE and nCR between fluorescent and nonfluorescent samples.

Association Between Intraoperative Fluorescence and Neuropathological Parameters

A total of 124 biopsy specimens was collected in the 11 patients with a newly diagnosed GBM. Of these, 86 specimens (69.4% of all samples) had an observable intraoperative red fluorescence, whereas in 38 (30.6% of all samples) there was no observable fluorescence. Of the 86 specimens with observable fluorescence, 82 were positive for the presence of tumor cells (95.3% of fluorescent specimens); 3 (3.5%) were either fully necrotic or showed abnormal, prominent vasculature; and 1 (1.2%) showed no abnormalities. Of the 38 nonfluorescent specimens, 28 (73.7% of nonfluorescent specimens) were positive for the presence of tumor cells; 8 (21.1%) were either fully necrotic or showed abnormal, prominent vasculature, or reactive gliosis; and 2 (5.3%) showed no abnormalities.

In this study, the PPV of observable intraoperative PpIX fluorescence (that is, the probability that tissue with observable intraoperative PpIX fluorescence is a true positive for the presence of tumor cells) was 0.95 (95% CI 0.88–0.98), whereas the NPV (that is, the probability that tissue without observable intraoperative PpIX fluorescence is a true negative for the presence of tumor cells) was 0.26 (95% CI 0.14–0.43). The sensitivity of observable intraoperative PpIX fluorescence (that is, the probability of observable intraoperative fluorescence given the presence of tumor cells in the tissue) was 0.75 (95% CI 0.65–0.82), whereas the specificity (that is, the probability of no observable intraoperative fluorescence given that there are no tumor cells in the tissue) was 0.71 (95% CI 0.42–0.90). An OR of 7.32 (95% CI 2.13–25.21; $p < 0.001$) for tissue with intraoperative PpIX fluorescence to be tumor compared with nonfluorescent tissue further summarizes and confirms the statistically significant association between observable intraoperative fluorescence and tumor tissue. Furthermore, 98.8% of fluorescent tissue (85 of 86 fluorescent specimens) was abnormal; that is, neoplastic, fully necrotic, or positive for abnormal, prominent vasculature. The corresponding PPV of observable intraoperative PpIX fluorescence for abnormal tissue was 0.99 (95% CI 0.93–1.00).

To test for the significance of the association between fluorescence levels (0–3) and the three neuropathological parameters under study, chi-square statistics and p values were calculated (Table 3). Each biopsy specimen was grouped based on its level of fluorescence (0–3), histopathological score (0–IV), tumor burden (0–III), and necrotic burden (0–III) in 2-way tables of association. The chi-square statistic for fluorescence and histopathological score was 58.8 ($p < 0.001$); for fluorescence and tumor burden it was 42.7 ($p < 0.001$); and for fluorescence and necrotic burden it was 30.9 ($p < 0.001$).

As histopathological score or tumor burden for a specimen increased (that is, histopathological scores from 0 to IV or tumor burden scores from 0 to III), the proportion of fluorescent samples as well as the levels of fluorescence (scores from 0 to 3) also increased (Fig. 3). To quantify this relationship, a Spearman rank correlation analysis was performed, producing a correlation coefficient of 0.51 ($p < 0.001$) for fluorescence and histopathological score, and 0.49 ($p < 0.001$) for fluorescence and tumor burden. No statistically significant correlation was observed between levels of fluorescence and necrotic burden by this statistical measure (the Spearman rank correlation coefficient was −0.02; $p = 0.79$).

Discussion

We report the initial findings from coregistered ALA-induced PpIX fluorescence-enhanced resection of malignant gliomas in 11 patients with newly diagnosed GBM, with the goal of establishing the statistical significance of relationships between 1) quantitative assessments of MR image signals and the spatially coregistered qualitative fluorescence signatures determined intraoperatively, and 2) these same qualitative fluorescence determinations and the subsequent neuropathological evaluations of the biopsy specimens taken from these locations. Previous studies of ALA-induced PpIX fluorescence have reported encouraging results in guiding the neurosurgeon to achieve higher percentages of complete tumor resection,28,29 which has repeatedly been shown to correlate with patient survival.1,2,17,24,29,30 Although pioneering in scope, intent, and positive outcome for high-grade glioma surgery, those studies did not explicitly describe quantitatively (either spatially or in terms of preoperative MR image contrast characteristics) the relationship between the MR imaging signature and the degree of intraoperative PpIX fluorescence observed by the neurosurgeon.

One standard feature used to distinguish pathological tissue pre- and postsurgically is contrast enhancement on MR imaging after Gd injection. In this study we used two measures to quantify contrast enhancement on T1-weighted image volumes: 1) GdE from subtraction image volumes (pre- and postcontrast injection), and 2) nCRs on T1-weighted, postcontrast-injection image volumes. The GdE served as a surrogate measure for Gd proper–induced changes in the MR images, whereas nCR served as a surrogate measure for what the neurosurgeon most often uses in the operating room on T1-weighted, Gd-enhanced images. We found evidence of a significant difference in both GdE and nCR between fluorescing and nonfluorescing tissues. The PpIX fluorescence can provide the neurosurgeon with real-time information for differentiating tumor from normal tissue, independent of any image-guidance system. The degree to which preoperative MR image signatures are predictive of intraoperative PpIX fluorescence is of practical importance in understanding the potential role of fluorescence during surgery.

In this study, the odds ratio for intraoperative fluorescence for tumor tissue was highly favorable (OR 7.32). The PPV for tissue with observable fluorescence to be tumor confirmed the effective accumulation of PpIX in tumor tissue (95%) and abnormal tissue (99%). The sensitivity and specificity measures of intraoperative fluorescence for tumor

tissue were also favorable (75 and 71%, respectively). Similar to previous studies, intraoperative macroscopic fluorescence showed sensitivity limitations. Low NPVs (26%) point to the need for improving the detection limit of intraoperative fluorescence imaging. Several groups, including ours, are using intraoperative probes that take advantage of the spectroscopic signature of PpIX (or similar fluorophores) and have signal detection sensitivities that exceed those of the current surgical microscope.3,9,28,29,36,38,40

Selective accumulation of PpIX in neoplastic tissues may involve changes in intracellular metabolism, increased ALA uptake, vascularization, proliferation, differentiation, or blood-brain barrier breakdown.4 Here, histopathological scores used pathological characteristics to categorize specimens into four distinct levels, in a manner similar to WHO grading of a surgical specimen. This analysis provided a semiquantitative assessment, analogous to histopathological grading, of the biological aggressiveness of each specimen, and accounted for other biological characteristics such as degree of differentiation, cellular metabolism, and environmental changes. Tumor burden scores offered another important metric, analogous to tumor infiltration, which was used to relate levels of fluorescence to the presence of tumor cells. These parameters were chosen in our analysis because previous studies have indicated that mitochondrial content and cellular density play a significant role in the selective accumulation of PpIX.4 An analysis of association performed using chi-square statistics demonstrated a significant relationship between the levels of intraoperative fluorescence and histopathological score ($\chi^2 = 58.8$, $p < 0.001$), between fluorescence and tumor burden ($\chi^2 = 42.7$, $p < 0.001$), and between fluorescence and necrotic burden ($\chi^2 = 30.9$, $p < 0.001$). The Spearman rank correlation analysis provided statistically significant correlation coefficients of 0.51 for fluorescence and histopathological score, and 0.49 for fluorescence and tumor burden, but no statistically significant correlation between fluorescence and necrotic burden. This lack of a direct correlation between degree of fluorescence and necrosis could be attributed to poor fluorescence in heavily necrotic tissue as a result of fewer viable PpIX-producing cells.

The neuropathological analysis increases confidence in the accuracy of intraoperative PpIX fluorescence for abnormal tissue. The data support the idea that biological aggressiveness and burden of tumor cells are important, synergistic factors that explain accumulation of PpIX to observable levels. This study uses parameters similar to conventional histopathological characteristics to provide explanatory variables for the selective accumulation of PpIX in resected tumor tissue. These results provide a framework for further understanding of PpIX fluorescence, as observed intraoperatively, relative to conventional notions of tumor grading and infiltration.

The Spearman rank correlation coefficients for histopathological score (0.51) and tumor burden (0.49), however, indicate that although these variables are important in understanding accumulation of PpIX, other biological characteristics, such as levels of cellular growth, endothelial proliferation, blood-brain barrier disruption, and possibly glial-cell phenotype are also likely to be important.4,7,11

This study adds two major contributions to the neurosurgical literature regarding FGR that differ from previous clinical studies in which PpIX fluorescence guidance was used. First, this work provides evidence that a strong correlation exists between features on preoperative MR imaging by using patient-specific image-guidance spatial information and intraoperative fluorescence, to the degree that spatially coregistered features on MR imaging are predictive of corresponding intraoperative fluorescence. Second, this work reports that a strong correlation exists between tumor aggressiveness and corresponding intraoperative fluorescence (using patient-specific image-guidance spatial information for each biopsy specimen), to the degree that spatially coregistered intraoperative PpIX fluorescence is

predictive of tumor aggressiveness. These contributions are of practical importance for the neurosurgical community to integrate FGR into conventional image-guidance protocols.

One limitation of our study is registration error of our image-guidance system and intraoperative brain shift and deformation, with subsequent degradation of navigational accuracy over the course of a surgical procedure. In an attempt to reduce errors in analysis that occur as a result of navigational inaccuracies, we constrained data points by using an ROI methodology. Although this methodology reduces this error, it does not completely eliminate it. Second, determination of intraoperative fluorescence in this study is nonquantitative, as it is in all current commercial adaptations of operating microscope systems. Quantitative determination of fluorescence will refine our understanding of the relationship, so that a standard can be applied between patients and across studies. Our group is actively working on this challenge. Furthermore, our group is currently developing a methodology to merge our fluorescence information with our stereovision system34 to create 3D surface maps of the surgical field, with fluorescence map overlays of these reconstructions onto the MR image-guidance cross-sectional images, using both qualitative and quantitative fluorescence information. Third, current fluorescence surgical systems are sometimes not able to detect low levels of fluorescence (for example, NPV 26%), which can lead to a high number of false negatives, as was observed in this study (that is, low NPVs). We have developed and are currently in clinical testing phases of an intraoperative probe that quantifies PpIX levels at submicrogram per milliliter concentrations, with the aim of distinguishing normal from abnormal tumor tissue in a more sensitive manner than is possible with our current fluorescence surgical microscope. Last, current fluorescence systems detect only fluorescence of surface tissue. Overlying nonfluorescent tissue, including blood or necrotic debris, will prevent visualization of deeper, fluorescing tumor. Systems capable of detecting fluorescing tissue at depth are also under development.

Conclusions

Analysis of our initial clinical experience with coregistered ALA-induced PpIX fluorescence–guided tumor resection in 11 patients with newly diagnosed GBM provides evidence of a significant relationship between Gd-induced contrast enhancement on preoperative MR imaging and observable intraoperative PpIX fluorescence. Furthermore, in newly diagnosed GBM, a strong relationship exists between tumor aggressiveness and observable fluorescence. In this study, intraoperative observable fluorescence was shown to have an excellent PPV, but a low NPV. This points to the usefulness and promise of this technology for tumor tissue identification, but also to the need for more sensitive fluorescence-detection systems. This study reports on the relationships between intraoperative fluorescence and histopathological characteristics analogous to important clinical parameters such as tumor grade and tumor infiltration. It is part of a larger effort to integrate conventional neuronavigational image guidance with fluorescence guidance to increase the probability and consistency of achieving maximal tumor resection.

Acknowledgments

Disclosure This research was supported in part by National Institutes of Health Grant Nos. R01NS052274-01A2 and K25CA138578. The authors acknowledge the support of Carl Zeiss Surgical GmbH (Oberkochen, Germany) and Medtronic Navigation (Louisville, CO) for use of the OPMI Pentero operating microscope and StealthStation Treon navigation system, respectively. The authors also acknowledge DUSA Pharmaceuticals (Tarrytown, NY) for supplying the ALA. Dr. Roberts serves on the Data Monitoring Committee for an unrelated Medtronic deep brain stimulation study.

Abbreviations used in this paper

ALA	δ-aminolevulinic acid
ALP	alkaline phosphatase
ALT	alanine aminotransferase
AST	aspartate aminotransferase
FGR	fluorescence-guided resection
GBM	glioblastoma multiforme
GdE	Gd-enhanced signal intensity
nCR	normalized contrast ratio
NPV	negative predictive value
PpIX	protoporphyrin IX
PPV	positive predictive value
ROI	region of interest

References

1. Albert FK, Forsting M, Sartor K, Adams HP, Kunze S. Early postoperative magnetic resonance imaging after resection of malignant glioma: objective evaluation of residual tumor and its influence on regrowth and prognosis. Neurosurgery. 1994; 34:45–61. [PubMed: 8121569]
2. Barker FG II, Prados MD, Chang SM, Gutin PH, Lamborn KR, Larson DA, et al. Radiation response and survival time in patients with glioblastoma multiforme. J Neurosurg. 1996; 84:442–448. [PubMed: 8609556]
3. Bogaards A, Varma A, Collens SP, Lin A, Giles A, Yang VX, et al. Increased brain tumor resection using fluorescence image guidance in a preclinical model. Lasers Surg Med. 2004; 35:181–190. [PubMed: 15389738]
4. Collaud S, Juzeniene A, Moan J, Lange N. On the selectivity of 5-aminolevulinic acid-induced protoporphyrin IX formation. Curr Med Chem Anticancer Agents. 2004; 4:301–316. [PubMed: 15134506]
5. Eljamel MS, Goodman C, Moseley H. ALA and Photofrin fluorescence-guided resection and repetitive PDT in glioblastoma multiforme: a single centre Phase III randomised controlled trial. Lasers Med Sci. 2008; 23:361–367. [PubMed: 17926079]
6. Fitzmaurice, GM.; Laird, NM.; Ware, JH. Applied Longitudinal Analysis. John Wiley & Sons; Hoboken, NJ: 2004.
7. Friesen SA, Hjortland GO, Madsen SJ, Hirschberg H, Engebraten O, Nesland JM, et al. 5-Aminolevulinic acid-based photo dynamic detection and therapy of brain tumors (review). Int J Oncol. 2002; 21:577–582. [PubMed: 12168102]
8. Hefti M, von Campe G, Moschopulos M, Siegner A, Looser H, Landolt H. 5-aminolevulinic acid induced protoporphyrin IX fluorescence in high-grade glioma surgery: a one-year experience at a single institutuion. Swiss Med Wkly. 2008; 138:180–185. [PubMed: 18363116]
9. Ishihara R, Katayama Y, Watanabe T, Yoshino A, Fukushima T, Sakatani K. Quantitative spectroscopic analysis of 5-aminolevulinic acid-induced protoporphyrin IX fluorescence intensity in diffusely infiltrating astrocytomas. Neurol Med Chir (Tokyo). 2007; 47:53–57. [PubMed: 17317941]
10. Kajimoto Y, Kuroiwa T, Miyatake S, Ichioka T, Miyashita M, Tanaka H, et al. Use of 5-aminolevulinic acid in fluorescence-guided resection of meningioma with high risk of recurrence. Case report. J Neurosurg. 2007; 106:1070–1074. [PubMed: 17564181]

11. Kennedy JC, Marcus SL, Pottier RH. Photodynamic therapy (PDT) and photodiagnosis (PD) using endogenous photosensitization induced by 5-aminolevulinic acid (ALA): mechanisms and clinical results. J Clin Laser Med Surg. 1996; 14:289–304. [PubMed: 9612195]
12. Koc K, Anik I, Cabuk B, Ceylan S. Fluorescein sodium-guided surgery in glioblastoma multiforme: a prospective evaluation. Br J Neurosurg. 2008; 22:99–103. [PubMed: 18224529]
13. Kremer P, Mahmoudreza F, Ding R, Pritsch M, Zoubaa S, Frei E. Intraoperative fluorescence staining of malignant brain tumors using 5-aminofluorescein-labeled albumin. Neurosurgery. 2009; 64(3 Suppl):53–61. [PubMed: 19240573]
14. Kuroiwa T, Kajimoto Y, Ohta T. Comparison between operative findings on malignant glioma by a fluorescein surgical microscopy and histological findings. Neurol Res. 1999; 21:130–134. [PubMed: 10048072]
15. Kuroiwa T, Kajimoto Y, Ohta T. Development of a fluorescein operative microscope for use during malignant glioma surgery: a technical note and preliminary report. Surg Neurol. 1998; 50:41–49. [PubMed: 9657492]
16. Kuroiwa T, Kajimoto Y, Ohta T. Surgical management for supratentorial astrocytic tumors. Minim Invasive Neurosurg. 1999; 42:182–186. [PubMed: 10667822]
17. Lacroix M, Abi-Said D, Fourney DR, Gokaslan ZL, Shi W, DeMonte F, et al. A multivariate analysis of 416 patients with glioblastoma multiforme: prognosis, extent of resection, and survival. J Neurosurg. 2001; 95:190–198. [PubMed: 11780887]
18. Louis DN, Ohgaki H, Wiestler OD, Cavenee WK, Burger PC, Jouvet A, et al. The 2007 WHO classification of tumours of the central nervous system. Acta Neuropathol. 2007; 114:97–109. [PubMed: 17618441]
19. Miyatake S, Kuroiwa T, Kajimoto Y, Miyashita M, Tanaka H, Tsuji M. Fluorescence of non-neoplastic, magnetic resonance imaging-enhancing tissue by 5-aminolevulinic acid: case report. Neurosurgery. 2007; 61:E1101–E1104. [PubMed: 18091261]
20. Moore GE, Peyton WT, French LA, Walker WW. The clinical use of fluorescein in neurosurgery: the localization of brain tumors. J Neurosurg. 1948; 5:392–398. [PubMed: 18872412]
21. Morofuji Y, Matsuo T, Hayashi Y, Suyama K, Nagata I. Usefulness of intraoperative photodynamic diagnosis using 5-aminolevulinic acid for meningiomas with cranial invasion: technical case report. Neurosurgery. 2008; 62(3 Suppl 1):102–104. [PubMed: 18424972]
22. Murray KJ. Improved surgical resection of human brain tumors: Part I. A preliminary study. Surg Neurol. 1982; 17:316–319. [PubMed: 6283688]
23. Okuda T, Kataoka K, Taneda M. Metastatic brain tumor surgery using fluorescein sodium: technical note. Minim Invasive Neurosurg. 2007; 50:382–384. [PubMed: 18210365]
24. Pichlmeier U, Bink A, Schackert G, Stummer W. Resection and survival in glioblastoma multiforme: an RTOG recursive partitioning analysis of ALA study patients. Neuro Oncol. 2008; 10:1025–1034. [PubMed: 18667747]
25. Pijl ME, Doornbos J, Wasser MN, van Houwelingen HC, Tollenaar RA, Bloem JL. Quantitative analysis of focal masses at MR imaging: a plea for standardization. Radiology. 2004; 231:737–744. [PubMed: 15163813]
26. Shinoda J, Yano H, Yoshimura S, Okumura A, Kaku Y, Iwama T, et al. Fluorescence-guided resection of glioblastoma multiforme by using high-dose fluorescein sodium. Technical note. J Neurosurg. 2003; 99:597–603. [PubMed: 12959452]
27. Stepp H, Beck T, Pongratz T, Meinel T, Kreth FW, Tonn JCh, et al. ALA and malignant glioma: fluorescence-guided resection and photodynamic treatment. J Environ Pathol Toxicol Oncol. 2007; 26:157–164. [PubMed: 17725542]
28. Stummer W, Novotny A, Stepp H, Goetz C, Bise K, Reulen HJ. Fluorescence-guided resection of glioblastoma multiforme by using 5-aminolevulinic acid-induced porphyrins: a prospective study in 52 consecutive patients. J Neurosurg. 2000; 93:1003–1013. [PubMed: 11117842]
29. Stummer W, Pichlmeier U, Meinel T, Wiestler OD, Zanella F, Reulen HJ. Fluorescence-guided surgery with 5-aminolevulinic acid for resection of malignant glioma: a randomised controlled multicentre phase III trial. Lancet Oncol. 2006; 7:392–401. [PubMed: 16648043]

30. Stummer W, Reulen HJ, Meinel T, Pichlmeier U, Schumacher W, Tonn JC, et al. Extent of resection and survival in glioblastoma multiforme: identification of and adjustment for bias. Neurosurgery. 2008; 62:564–576. [PubMed: 18425006]

31. Stummer W, Reulen HJ, Novotny A, Stepp H, Tonn JC. Fluorescence-guided resections of malignant gliomas—an overview. Acta Neurochir Suppl. 2003; 88:9–12. [PubMed: 14531555]

32. Stummer W, Stepp H, Möller G, Ehrhardt A, Leonhard M, Reulen HJ. Technical principles for protoporphyrin-IX-fluorescence guided microsurgical resection of malignant glioma tissue. Acta Neurochir (Wien). 1998; 140:995–1000. [PubMed: 9856241]

33. Stummer W, Stocker S, Wagner S, Stepp H, Fritsch C, Goetz C, et al. Intraoperative detection of malignant gliomas by 5-aminolevulinic acid-induced porphyrin fluorescence. Neurosurgery. 1998; 42:518–526. [PubMed: 9526986]

34. Sun H, Roberts DW, Farid H, Wu Z, Hartov A, Paulsen KD. Cortical surface tracking using a stereoscopic operating microscope. Neurosurgery. 2005; 56(1 Suppl):86–97. [PubMed: 15799796]

35. Utsuki S, Miyoshi N, Oka H, Miyajima Y, Shimizu S, Suzuki S, et al. Fluorescence-guided resection of metastatic brain tumors using a 5-aminolevulinic acid-induced protoporphyrin IX: pathological study. Brain Tumor Pathol. 2007; 24:53–55. [PubMed: 18095131]

36. Utsuki S, Oka H, Miyajima Y, Shimizu S, Suzuki S, Fujii K. Auditory alert system for fluorescence-guided resection of gliomas. Neurol Med Chir (Tokyo). 2008; 48:95–98. [PubMed: 18296881]

37. Utsuki S, Oka H, Sato S, Shimizu S, Suzuki S, Tanizaki Y, et al. Histological examination of false positive tissue resection using 5-aminolevulinic acid-induced fluorescence guidance. Neurol Med Chir (Tokyo). 2007; 47:210–214. [PubMed: 17527047]

38. Utsuki S, Oka H, Sato S, Suzuki S, Shimizu S, Tanaka S, et al. Possibility of using laser spectroscopy for the intraoperative detection of nonfluorescing brain tumors and the boundaries of brain tumor infiltrates. Technical note. J Neurosurg. 2006; 104:618–620. [PubMed: 16619668]

39. Valdés PA, Fan X, Ji S, Harris BT, Paulsen KD, Roberts DW. Estimation of brain deformation for volumetric image updating in protoporphyrin IX fluorescence-guided resection. Stereotact Funct Neurosurg. 2010; 88:1–10. [PubMed: 19907205]

40. Yang VX, Muller PJ, Herman P, Wilson BC. A multispectral fluorescence imaging system: design and initial clinical tests in intra-operative Photofrin-photodynamic therapy of brain tumors. Lasers Surg Med. 2003; 32:224–232. [PubMed: 12605430]

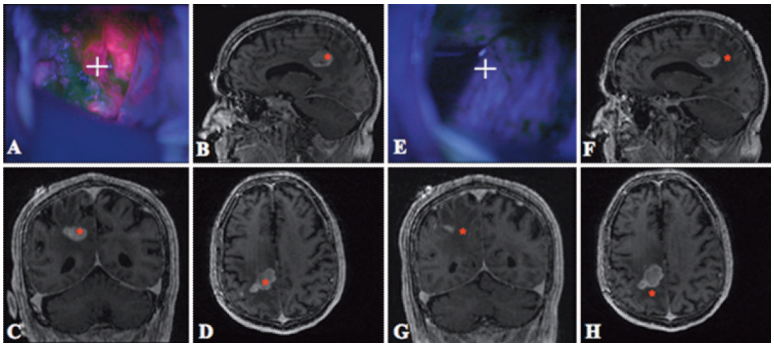

Fig. 1.

Case 3. Images of a right parietal lesion. **A**: During resection, the surgical cavity displayed a high level of PpIX fluorescence *(red)* at the focal point of the surgical microscope *(white cross hairs)*. **B–D**: Navigational information localized the focal point to an area of high contrast enhancement (*red asterisks* on MR images). **E**: Later during resection, the focal point of the operating microscope *(white cross hairs)* is focused on tissue with no observable PpIX fluorescence. **F–H**: Navigational information localized the focal point to an area without contrast enhancement *(red asterisks)*.

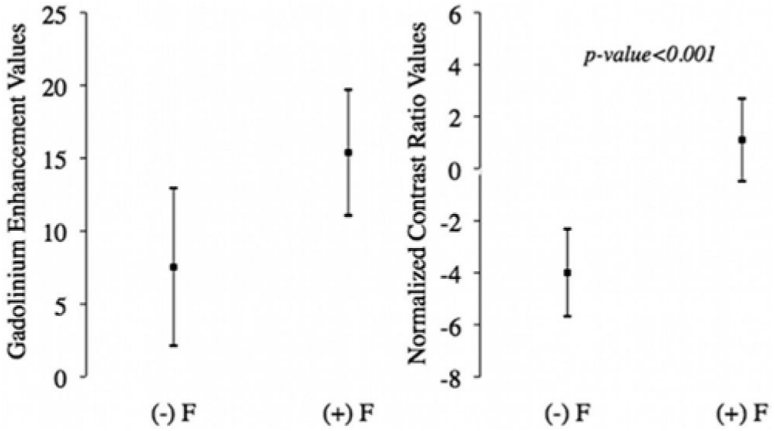

Fig. 2.

Diagrams of the 95% CIs of the mean of MR image measures. **Left**: The 95% CIs of the mean for the GdE values from subtraction images of both fluorescent ([(+) F]; 57 samples, mean 15.38, 95% CI 11.07–19.69) and nonfluorescent ([(−) F]; mean 7.54, 95% CI 2.14–12.94) groups (random-effects, mixed model: mean difference 8.33, 95% CI 1.42–15.24; $p = 0.018$). **Right**: The 95% CIs of the mean for the nCR of both fluorescent (77 samples, mean 1.10, 95% CI −0.49 to 2.69) and nonfluorescent (mean −3.99, 95% CI −5.67 to −2.32) groups (random-effects, mixed model: mean difference 5.15, 95% CI 2.54–7.77; $p < 0.001$). The *small black square* in the middle of the *vertical line* represents the mean, and the *whiskers* represent the upper and lower 95% confidence limits of the mean.

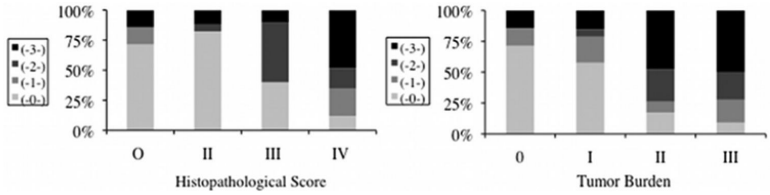

Fig. 3.

Percentage bar graphs of fluorescence and neuropathological parameters. A relationship between qualitative fluorescence levels (0–3) and the two neuropathological parameters was observed. The Spearman rank correlation was 0.51 ($p < 0.001$) for the correlation between fluorescence and histopathological score **(left)**, and 0.49 ($p < 0.001$) for the correlation between fluorescence and tumor burden **(right)**.

TABLE 1

Summary of characteristics in 11 patients with a newly diagnosed GBM

Case No.	Age (yrs), Sex	Side	Location	Enhancing Tumor Vol (cm^3)
1	61, M	lt	temporoparietal	19.5
2	52, M	rt	temporal	98.4
3	80, M	rt	parietal	8.7
4	55, F	lt	parietal	44.8
5	68, M	lt	parietal	35.1
6	60, M	lt	frontotemporal	40.7
7	76, F	rt	parietal	31.7
8	59, M	lt	temporal	46.3
9	76, F	lt	temporal	4.4
10	60, M	lt	temporoparietal	4.2
11	55, M	rt	occipitoparietal	35.9

TABLE 2

Statistical measures used to summarize the predictive relationship for PplX fluorescence and tissue histopathology*

Factor	Neoplastic Tissue
sensitivity	0.75 (0.65–0.82)
NPV	0.26 (0.14–0.43)
specificity	0.71 (0.42–0.90)
PPV	0.95 (0.88–0.98)
OR	7.32 (2.13–25.21)

*Values in parentheses denote the 95% CIs

TABLE 3

Two-way tables of association for tissue biopsy samples obtained in patients newly diagnosed with GBM*

Fluoressence Score	Histopathological Score				Tumor Burden				Necrotic Burden				Totals
	0	II	III	IV	0	I	II	III	0	I	II	III	
0	10 (76)	14 (14.8)	4 (0.3)	10 (9.4)	10 (7.6)	19 (7.8)	4 (1.3)	5 (8.1)	24 (19.3)	2 (10.1)	1 (1.5)	11 (7.0)	38
1	2 (0.1)	0 (2.9)	0 (1.7)	19 (1.7)	2 (0.1)	7 (0.4)	2 (0.9)	10 (0.1)	6 (10.7)	7 (5.6)	0 (0.8)	8 (3.9)	21
2	0 (2.3)	1 (1.1)	5 (7.1)	14 (0.0)	0 (2.3)	2 (2.1)	6 (1.4)	12 (1.2)	13 (10.2)	4 (5.3)	1 (0.8)	2 (3.7)	20
3	2 (1.9)	2 (2.8)	1 (1.9)	40 (3.2)	2 (1.9)	5 (4.1)	11 (0.8)	27 (2.8)	20 (22.9)	20 (12.0)	3 (1.8)	2 (8.3)	45
totals	14	17	10	83	14	33	23	54	63	33	5	23	124
	$\chi^2 = 58.8$†				$\chi^2 = 42.7$†				$\chi^2 = 30.9$†				

*Tissue biopsy samples were grouped according to their neuropathological parameter scores and fluorescence level (expected calculated values for each cell are given in parentheses).

†A chi-square statistical analysis was used to assess whether there was a significant association between fluorescence and the neuropathological parameter scores ($p < 0.001$ for all omparisons).